

Study of Thermal Activated CO₂ Extraction Processes from Carbonate Apatites Using Gas Chromatography

V.N. Kuznetsov^{1,*}, A.A. Yanovska^{1,†}, S.V. Novikov¹, V.V. Starikov², T.G. Kalinichenko¹, A.V. Kochenko¹,
A.G. Ryabyshev¹, Ya.V. Khyzhnya, S.N. Danilchenko^{1,‡}

¹ Institute of Applied Physics of NASU, 58, Petropavlovskaya Str., 40000 Sumy, Ukraine

² NTU "Kharkiv Politechnological Institute", 21, Frunze Str., 61002 Kharkiv, Ukraine

³ Sumy State University, 2, Rimsky-Korsakov Str., 40007 Sumy Ukraine

(Received 19 February 2015; published online 20 October 2015)

The study of carbonate in the structure of carbonate-containing apatites (CCA) is an actual problem due to the similarity of such systems to natural apatites of mammalian bone tissue. The search of the optimal synthesis procedures was also carried out in order to obtain carbonate apatites with the highest rate of incorporation of carbonate ions in the apatite structure.

The analysis of carbonate-group temperature behavior in apatites of various origin helps to understand their structural and functional roles in biologically relevant apatite materials. The thermal extraction and accumulation of CO₂ from biogenic and geological apatites is also of interest for the further carbon isotope analysis with accelerating mass-spectrometry. X-ray diffraction analysis, infrared spectroscopy and scanning electron microscopy as well as self-proposed gas chromatography method with thermo-programmed probe extraction were used for carbonate temperature behavior study. This new method allows determining CO₂ concentration released from CCA during annealing. The defined changes in the carbonate apatite structure depending on the synthesis procedure were observed.

Keywords: Carbonate apatite, Carbonate, X-Ray diffraction analysis, Infrared spectroscopy, Gas chromatography, TECR.

PACS numbers: 87.85.J –, 87.64.Bx, 87.64.km

1. INTRODUCTION

The need to study the forms of carbonate presence in both the fundamental mineral component of skeleton tissues ("physiological apatites") and many ectopic formations ("pathological apatites") is caused by the fact that all kinds of biological apatites are carbonate-containing [1-6]. Undoubtedly, an important functional area of the above mentioned element in apatites of biological tissues is behind this.

Solubility of biogenic and synthetic carbonate-containing apatites (CCA) is proportional to the carbon concentration therein, and this functional relationship is obvious in consideration of biological systems: carbonate content is high in the bone tissue bioapatite (4.8 %) demanding a continuous restructuring and renovation, and is slightly lower in the tooth enamel apatite (3 %) which is the most stable and chemically resistant body tissue [7, 8].

However, the presence of carbon in bioapatites is not limited only by solubility control, but, evidently, is multifunctional and closely associated with the most important biochemical and physiological processes. This is confirmed by various types of positioning of carbon-containing ions and molecules in biogenic and synthetic apatites [5, 7, 9] as well as by their ability to mutual migrations and transformations. Migration processes of carbonates and their transition to the gas phase in the form of CO₂ when heated or annealed are conditioned by both the structural and morphological features of certain CCA and preferred localization of their carbon component. Therefore, the study of the temperature behavior of carbonates in apatites

of different origin facilitates the understanding of their structural and functional role in various biologically relevant apatite materials.

Moreover, the thermal extraction and accumulation of CO₂ from biogenic and natural (geological) apatites are also of interest for the subsequent carbon isotope analysis using accelerating mass-spectrometry (AMS). The results of this study give information about the age of the natural object and its origin. The possible affiliation of the carbonate component extracted for the analysis in the form of CO₂ to the structure of the initial mineral is the key question in this case. The problem is complicated by multivariance of carbon localization in apatites.

As shown in many publications [5, 7-9], CO₃²⁻ ion can be both the component of the crystal structure replacing PO₄³⁻ and/or OH⁻ that leads to the formation of carbonate-apatite of the B- or A-type, respectively, [10] and present on the surface and in the near-surface layers of the crystals (in the "non-apatite environment" [5]).

From general considerations, it is clear that CO₃²⁻ ions located directly in the structure of apatite crystals are more suitable for determining the radiocarbon age than adsorbed carbonates of the surface localization, although this assumption requires rigorous justification. Undoubtedly, the fitting of correct modes of CO₂ thermal extraction from apatites is one of the determining factors of a reliable determination of the radiocarbon age of the mineral. Moreover, a strong belief in the necessity of preliminary studies of the temperature destruction behavior of the probe with gaseous CO₂ extraction has developed among a narrow circle of specialists associated with the

* vkuznetsov.ua@gmail.com

† biophy@yandex.ua

‡ danilsergej@yandex.ua

development of methods for preparation of the carbon probe of apatite origin for the AMS analysis.

The aim of the present work consisted in developing new methods of study of the thermal activated processes of gaseous CO_2 extraction from carbonate apatites of different origin. Review of the current state of the question is performed based on both the analysis of the available literature data and experience of our previous studies. Because of the inaccessibility and, partly, the lack of suitability of the standard commercial equipment for the thermal analysis to solving the assigned tasks, the authors have to resort to the development and production of the necessary hardware, which should become the prototype of the next generation facilities.

Classical thermal analysis associated with the mass spectrometry, infrared spectroscopy, gas chromatography was used in numerous works [9, 11-13] for the study of thermal activated processes in carbonate apatites with extraction of gaseous products. Such instrumental methods as X-ray diffractometry, electron microscopy, electron paramagnetic resonance are applied, as a rule, for the control of the changes in the structural state of apatites due to heating. All the enumerated methods were used by different research groups in various combinations determined, first of all, by the accessibility of one or another technique and its instrumentation.

The optimal set of tools and methods, which allow to obtain with minimal cost reliable and sufficient information about the temperature transformations of carbonate apatites, has not still been determined. The multichannel registration is the advantage of the mass-spectrometric analysis of extracted gases (the evolved gas mass spectrometry) [14], which allows to simultaneously register in one process the temperature dependences of some volatile components (for example, CO_2 , CO , and H_2O). This gives the researcher a more complete picture of thermal transformations of the sample. However, taking into account the phenomena of discrimination typical for mass-spectrometry, the information obtained cannot be considered quantitative. On the other hand, a reliable quantitative determination of extracted CO_2 can be performed by the gas chromatography method (at a correct implementation of the calibration procedures), although in this case detection of other gas components causes serious methodological and instrumental difficulties.

In the present work, we have proposed and practically implemented the outline of direct analysis of the CO_2 extraction processes from carbonate apatites by applying gas chromatography method with thermo-programmed extraction of the probe. The methods of scanning electron microscopy with the X-ray microanalysis, X-ray diffractometry and infrared spectroscopy were used for the detailed characteristic of the synthesized samples of carbonate apatites.

2. MATERIALS AND METHODS

2.1 Synthesis

Nonstoichiometric apatites can be obtained by various deposition methods in a wide range of pH, temperatures and concentrations. It is difficult to control their crystalline characteristics and composition because of the presence of different substitutions in the lattice sites.

In the most common syntheses, $\text{Ca}(\text{NO}_3)_2$ or CaCl_2 are used as the source of calcium, and Na_2HPO_4 , NaH_2PO_4 or $(\text{NH}_4)_2\text{HPO}_4$ – as the source of phosphate ions. The carbonate ions are introduced by the addition of NaHCO_3 or $(\text{NH}_4)\text{HCO}_3$ depending on the chosen synthesis route. At that, sodium can be incorporated into the crystal lattice during the formation of carbonate apatites of the B- or AB-types [15].

In our work, synthetic carbonate apatites were prepared by the chemical deposition method with the addition to one of the initial solutions of sodium bicarbonate as the source of carbonate ions. The samples, hereinafter denoted as 1-6, were synthesized under similar conditions, however, the order of introduction of reagents to the chemical synthesis significantly differed (Fig. 1).

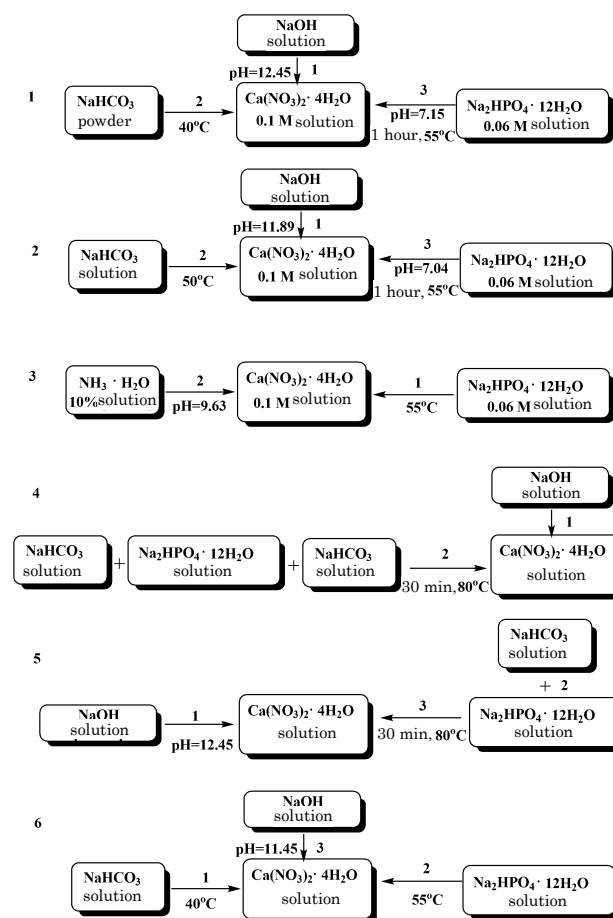
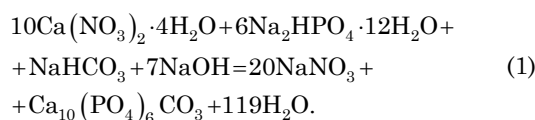


Fig. 1 – Synthesis schemes of the material based on carbonate apatite (1, 2, 4, 5, 6) and hydroxyapatite (HA) (synthesis 3)

Carbonate apatite is synthesized according to the following reaction equations:

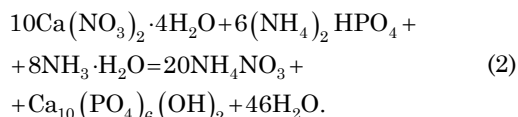


In **synthesis 1**, 10 % solution of NaOH was added to the solution $\text{Ca}(\text{NO}_3)_2 \cdot 4\text{H}_2\text{O}$ (0.1 mole/l) during heating to obtain pH = 12.5. At that, $\text{Ca}(\text{OH})_2$ sediment was formed, to which 0.84 g of NaHCO_3 powder were then added. After that, solution $\text{Na}_2\text{HPO}_4 \cdot 12\text{H}_2\text{O}$ (0.06 mole/l) was

dropwise added with constant mixing. pH of the initial solution decreased to 7.15 in this case.

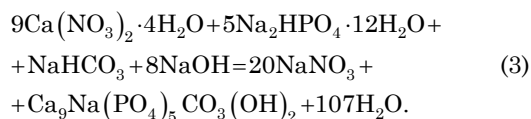
In **synthesis 2**, 10 % solution of NaOH was added to the solution Ca(NO₃)₂·4H₂O (0.1 mole/l) during heating. And 0.84 g of NaHCO₃ in the form of solution were added to the obtained sediment; at that, pH = 11.9. Then, solution Na₂HPO₄·12H₂O (0.06 mole/l) was dropwise added with constant mixing. pH of the initial solution decreased to 7.04 in this case.

Synthesis 3 was performed without the introduction of NaHCO₃ to obtain stoichiometric apatite (SHA) and comparison of its crystal structure with the carbonate apatites (CHA).



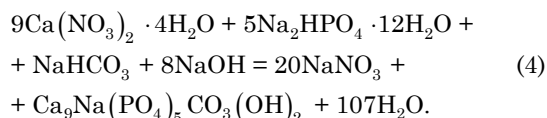
Solution (NH₄)₂HPO₄ (0.06 mole/l) was dropwise added with constant mixing to the solution Ca(NO₃)₂·4H₂O (0.1 mole/l) during heating. After that, 25 % solution of NH₃·H₂O was added to obtain pH = 9.5.

In **synthesis 4**, the order of introduction of reagents was changed. 0.84 g of sodium bicarbonate (in the form of solution) were added to the solution Na₂HPO₄·12H₂O (0.06 mole/l) and then added with constant mixing and during heating to the solution containing Ca(NO₃)₂·4H₂O (0.1 mole/l) and NaOH, as in the previous synthesis.



In **synthesis 5**, another order of introduction of reagents was used. 10 % solution of NaOH was added to the solution Ca(NO₃)₂·4H₂O (0.1 mole/l) during heating. Then, solution Na₂HPO₄·12H₂O (0.06 mole/l) with the solution NaHCO₃ (0.84 g) on top was dropwise added with constant mixing. The obtained sediment was more compressed in comparison with sediments in the above listed syntheses.

In **synthesis 6**, solution NaHCO₃ (0.84 g were dissolved in 20 ml of water) was added with constant mixing and heating to the solution Ca(NO₃)₂·4H₂O (0.1 mole/l). Then, solution Na₂HPO₄·12H₂O (0.06 mole/l) was dropwise added; pH of the obtained solution was adjusted to 11.75 by dropwise adding of 10 % solution of NaOH. The synthesis was carried out according to the following reaction equation:



The obtained sediments were aged during 2 or 7 days in order to establish the influence of the crystallization duration on their crystal structure.

The prepared samples hereinafter are called in compliance with the serial number of the synthesis variant. Samples 1, 4 and 2, 5 form couples different by the synthesis reaction equations. Thus, equation (1) corresponds to the samples 1 and 4, equation (3) – to 2 and 5.

2.2 Thermo-programmed gas probe extraction with chromatographic registration (TECR)

The experimental facility is intended to remove gases from solid samples by the thermal extraction method and determine their quantitative content. Structural scheme of the facility is illustrated in Fig. 2.

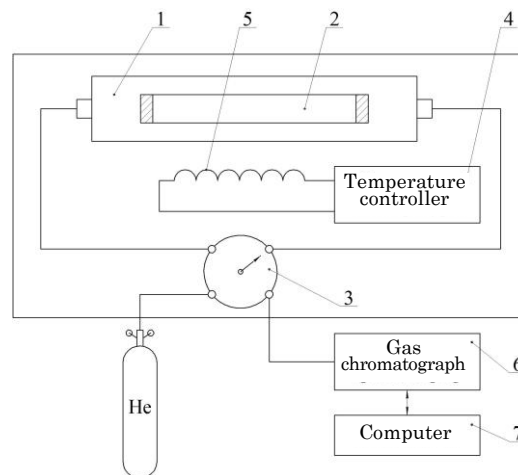


Fig. 2 – Structural scheme of the experimental facility

The facility consists of the thermal extraction oven and gas chromatograph. Thermal extraction oven is composed of the sealed vacuum reactor (1) heated by the heater (5), gas flow switch (3), temperature controller (4) with thermocouple control, and personal computer (7). Helium in a balloon with the concentration of 99.999 % is used as gas feed in the facility. Reactor is intended for loading the cell with a solid grinded sample, its sealing and gas emission. Gas evolution from the sample occurs in the closed volume of the reactor in the helium environment under the action of high temperatures.

The facility includes a gas chromatograph equipped with a thermal conductivity detector in order to register gases released during thermal extraction and determine their concentration. The process of sample heating, temperature stabilization in heating points, registration of the quantitative gas content is performed under the control of a personal computer by a specialized program.

The main task of the study is to measure the amount of carbon dioxide formed when carbonate escapes from the HA structure by the following technique.

1. The cell with the sample is placed into the reactor, which is hermetically sealed and evacuated by the backing pump to ~10 Pa during 10 minutes.

2. Extraction of carbon dioxide from the HA structure for further analysis is carried out by heating the sample during 10 minutes in each point in the temperature range from 600 °C to 1000 °C with the step of 40 °C.

3. The gas evolved at each stage is supplied to the separating column of gas chromatograph, where heating at 50 °C occurs during 3 minutes followed by the linear heating to 150 °C with the rate of 15 °/min. Registration of the carbon dioxide peak area is done on PC.

4. Calculation of the extracted gas concentration is performed by converting the CO₂ peak area to its volume. Then, evolved carbon dioxide volume was reduced to the weight of the studied sample of 1 g by the formula $V_{x1g} = V_x / M_x$, where V_x is the gas volume measured in the heating point; M_x is the sample mass.

2.3 Energy-dispersive elemental microanalysis (EDA)

Energy-dispersive elemental microanalysis was used to determine the elemental composition of the sample on a certain region of its surface applying energy-dispersive spectrometer involved in composition of the scanning electron microscope REMMA-102 (Selmi).

Samples in powder form were pressed by hand press in aluminum mandrels, which then were pasted on the metal plate with carbon sticky tape. A gold coating was sprayed on the samples by the vacuum plant VUP-5M (Selmi) to prevent the influence of electrostatic charge.

EDA was conducted by scanning over the sample area with 1000x magnification, accelerating voltage of 20 keV and probe current of 3 nA. Angle of extraction of characteristic X-ray radiation is 40°, exposure time is 200 s.

2.4 X-ray diffractometry (XRD)

The X-ray diffraction studies of the sample structure were carried out by using the automated diffractometer DRON-4-07 (Scientific Production Enterprise Burevestnik, www.bourestnik.ru). Automation system DRON-4 is based on the microprocessor controller which provides the control of goniometer GUR-9 and digital data transfer to PC.

CuK α radiation (wavelength 0.154 nm) and the Bragg-Brentano focusing θ - 2θ (2θ is the Bragg angle) were used in survey. The values of the current and voltage on the X-ray tube were equal to 20 mA and 40 kV, respectively. A survey of the samples was performed in the permanent record mode (rate 1 °/min), the range of angles 2θ from 10° to 60°.

The experimental results were transferred directly to the software package DifWin-1 ("Etalon-TTs" Co Ltd, www.specord.ru) for the preprocessing. Identification of the crystalline phases was carried out using the JCPDS (Joint Committee on Powder Diffraction Standards).

2.5 IR-spectroscopy (IRS)

The IR spectrometry is one of the most simple, efficient and widely used methods of analysis of substituted carbonate apatites. By analyzing the IR spectra, one can establish what kind of substitution occurred in the apatite structure.

Thus, the maximum at 878-880 cm^{-1} indicates the presence of CO_3^{2-} A-type substitutions. 1410, 1450 and 873 cm^{-1} are the typical absorption bands for the B-type carbonate apatite [16].

Increase in the carbonate content leads to the growth of the maximum intensity at 872 cm^{-1} . It is possible to determine the A/B carbonate ratio by the intensity of the corresponding maxima at 880 and 873 cm^{-1} [17]. Absorption band of 2344-2339 cm^{-1} corresponds to the asymmetrical valence vibrations of CO_2 .

In our work, the IRS was implemented in the range of 4000-400 cm^{-1} using IR spectrometer Spectrum One (PerkinElmer, www.perkinelmer.com). Grinded samples were mixed with KBr powder before measurements in the ratio of 2.5-3 mg of the sample per 300 mg of KBr and pressed into tablets.

3. RESULTS AND DISCUSSION

3.1 X-ray diffractometry

3.1.1 General description

In addition to the initial, the samples thermally treated at 600 and 900 °C during 1 hour were studied using X-ray diffractometry. Temperature data were chosen for several reasons. At 600 °C, there occurs the removal of adsorbed water and residual synthesis products, beginning of the recrystallization processes, output of carbonate localized in the near-surface layer of the sample [18]. Annealing at 900 °C leads to the recrystallization and, first of all, is used for the estimation of the initial apatite stoichiometry.

A qualitative X-ray diffraction analysis showed that HA ($\text{Ca}_5(\text{PO}_4)_3\text{OH}$, JCPDS 9-432) is the master phase in all the samples. One more phase – rhenanite (NaCaPO_4 , JCPDS 29-1193) is identified after thermal treatment in some of them (1, 4, 6, and, probably, 5) that is possible taking into account the features of its formation [19].

Diffraction patterns of the studied samples are illustrated in Fig. 3-Fig. 5. The main peaks of HA are denoted by the Miller indices, also the line diffraction pattern of HA JCPDS 9-432 is present on each picture. Symbol ● denotes one of the main peaks of rhenanite corresponding to the crystallographic plane (0 3 1).

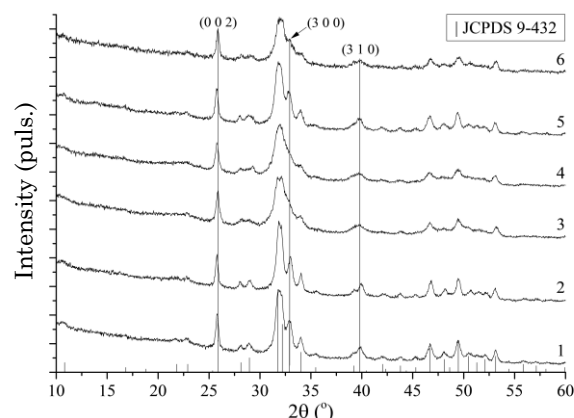


Fig. 3 – Diffraction patterns of the initial samples

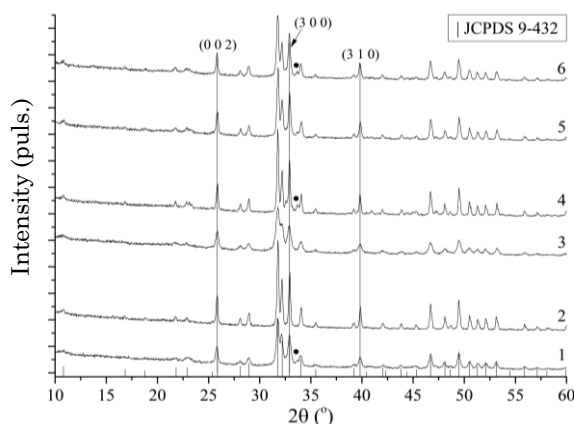


Fig. 4 – Diffraction patterns of the samples annealed at the temperature of 600 °C

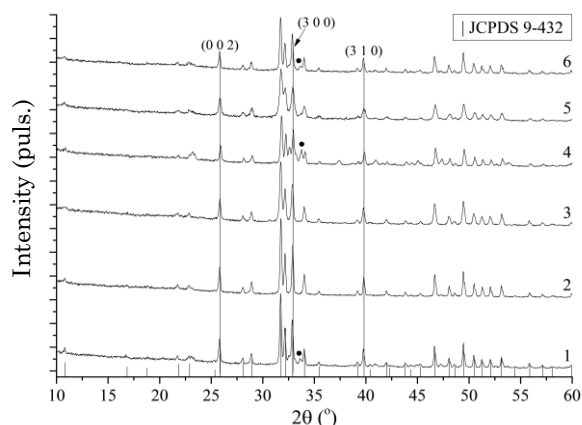


Fig. 5 – Diffraction patterns of the samples annealed at the temperature of 900 °C

A quantitative phase analysis was implemented by the method of alumina numbers [20]. Calculation of the average crystallite sizes in different planes was carried out by the Scherrer formula (plane (0 3 1) relates to rhenanite, others – to HA) [21]. Since HA lines (0 0 2) and (0 0 4) are well distinguished even in the initial samples, separation of the contributions of small-size crystallites and microstrain value to the peak broadening was performed by the approximation method [22].

Parameters of the apatite unit cell were calculated for all the samples, since their deviations from the standard values indicate structural imperfection caused also by the carbonate substitutions [23]. In the case of the initial samples, calculation was performed over the (2 1 0) and (0 0 4) planes. (4 1 0) and (0 0 4) planes were chosen for the thermally treated samples due to better separation of the peaks, since consistent errors including determination of the interplanar spacing decrease with increasing diffraction angle.

Structural and substructural parameters of the samples as well as the quantitative assessment of their phase composition are presented in Table 1-Table 3.

3.1.2 Initial samples

The largest displacement of the peaks (0 0 2), (3 0 0) and (3 1 0) is observed for the samples 2 and 5 compared with stoichiometric HA (sample 3) that indicates an increased imperfection of their structure caused, probably, by the presence of certain substitutions.

A more perfect crystal structure than in SHA is observed for the initial samples 1 and 2 that is confirmed not only by a better diffraction pattern (Fig. 3), but also by larger average crystallite sizes as well as lower microstrain values along the direction [0 0 c] (see Table 1). However, we should note that this fact is caused by other reasons, probably, synthesis features than the presence of carbonate ions in the HA structure, since any substitutions in the crystal lattice can only lead to the deterioration of crystallinity.

Crystallinity of the sample 5 is better than that of SHA, but one can observe its deterioration in the direction [0 0 c] caused by the decrease in the average crystallite size and increase in the microstrain.

Samples 4 and 6 show the diffraction pattern similar to the stoichiometric HA, however, a higher imperfection

is observed in the sample 4 than in the sample 3. In the case of the sample 6, the microstrain value corresponds to SHA at larger crystallite sizes.

3.1.3 Thermally treated samples

After thermal treatment at 600 °C during 1 hour all the CHA samples show better crystallinity than in SHA (especially for the samples 2, 4, and 5) due to better diffraction pattern and larger crystallite sizes. This can be caused by higher imperfection of the crystal structure of the initial samples (the higher imperfection of the initial samples, the less energy is necessary for the beginning of recrystallization) that, in turn, may be the result of incorporation to the lattice of HA carbonate ions. The last conclusion for the samples 2 and 5 is also confirmed by the TECR (Fig. 6).

Annealing at 900 °C is followed by the increase in the crystallinity of SHA, but, however, CHA samples behave differently. Thus, crystallinity of the samples 1 and 2 is higher than for SHA. Samples 4 and 5 possess a worse diffraction pattern and significantly smaller crystallite sizes in some planes. Sample 6 in whole corresponds to the sample 3 excepting the presence of rhenanite.

3.1.4 Substructural analysis

Analysis of (0 0 2) and (0 0 4) peak broadening shows that average crystallite size in all the initial carbonate-containing samples, except sample 5, is larger than in SHA. A similar trend is observed after thermal treatment at 600 °C except sample 1. Annealing at 900 °C results in a single value of crystallite sizes of ~ 40 nm.

Increase in the structure microstrain is observed for the samples 1 and 2 after annealing at 600 °C. Degree of imperfection is constant with increasing temperature to 900 °C. Samples 4 and 5 demonstrate the decrease in the lattice imperfection with increasing annealing temperature. Change in the microstrain value of the sample 6 is similar to that for the SHA – decrease after primary annealing followed by the increase. Such behavior can be caused by the incorporation of carbonate, which is present in the oven environment, into the sample structure during annealing at 900 °C.

3.2 Energy-dispersive elemental microanalysis

Analysis of the initial samples by the EDA method has shown the presence therein of calcium and phosphorus. Besides the given elements, sodium is also present in the sample 4 that correlates well with the results of the X-ray diffractometry indicating the formation in this sample of the greatest amount of the rhenanite phase after thermal treatment.

3.3 IR spectrometry

Analysis of the IR spectra (Fig. 6-Fig. 8) has revealed the presence in all the samples of the following absorption bands:

- 3000-3700 cm⁻¹ – valence vibrations of the hydroxyl group corresponding to water (adsorbed and included in the structure);
- 2850-2950 cm⁻¹ – valence vibrations ν_1 of the HPO₄²⁻ group;

Table 1 – Structural and substructural parameters of the initial samples

Sample	Phase composition		Crystallite sizes according to Scherrer, nm					Crystallite sizes and microstrain value		Parameters of the HA cell	
	HA, %	Rh, %	(0 0 2)	(2 1 0)	(3 0 0)	(0 3 1)	(0 0 4)	<i>L</i> , nm	ε , $\cdot 10^3$	a^1 , nm	c^2 , nm
1	100	–	30.4	17	17	–	31.3	29.4	0.177	0.943	0.689
2	100	–	30.2	19.3	20.5	–	28.1	32.6	0.426	0.94	0.69
3	100	–	24.4	13	–	–	22.3	26.8	0.645	0.943	0.688
4	100	–	24.4	18.2	–	–	19.9	31.5	1.6	0.931	0.689
5	100	–	27	12.9	17.2	–	33.9	22.4	1.3	0.944	0.69
6	100	–	28.7	–	–	–	25.7	32.4	0.697	–	0.689

Table 2 – Structural and substructural parameters of the samples annealed at 600 °C

Sample	Phase composition		Crystallite sizes according to Scherrer, nm					Crystallite sizes and microstrain value		Parameters of the HA cell	
	HA, %	Rh, %	(0 0 2)	(2 1 0)	(3 0 0)	(0 3 1)	(0 0 4)	<i>L</i> , nm	ε , 10^3	a^1 , nm	c^2 , nm
1	92.3	7.7	33.7	23.9	32.1	26.9	42.9	27.8	1.097	0.942	0.689
2	100	–	47.6	50.2	57	–	67.6	36.7	1.071	0.942	0.689
3	100	–	29.3	23.4	33.8	–	32	27.1	0.488	0.942	0.688
4	91	9	48.7	46	67	31	72.9	36.6	1171	0.942	0.688
5	100	–	40.4	41.7	50.1	–	48.4	34.8	0.7	0.942	0.688
6	93.7	6.3	44.5	36.9	51.1	40.4	42.9	46.3	0.145	0.942	0.689

Table 3 – Structural and substructural parameters of the samples annealed at 900 °C

Sample	Phase composition		Crystallite sizes according to Scherrer, nm					Crystallite sizes and microstrain value		Parameters of the HA cell	
	HA, %	Rh, %	(0 0 2)	(2 1 0)	(3 0 0)	(0 3 1)	(0 0 4)	<i>L</i> , nm	ε , 10^3	a^1 , nm	c^2 , nm
1	91.2	8.8	50.6	52.3	73	53.8	71.5	39.2	1	0.943	0.689
2	100	–	51.4	58.4	67.8	–	70.7	40.4	0.913	0.942	0.689
3	100	–	47.6	41.6	39.9	–	59.5	39.6	0.726	0.943	0.689
4	76	24	49	34.5	64.4	32.1	55.5	43.8	0.412	0.941	0.688
5	100	–	42.5	26	40.1	–	40.5	44.7	0.2	0.942	0.689
6	93	7	50.3	50	62.7	43.9	64.6	41.2	0.755	0.943	0.689

– 1640 cm^{-1} – deformation vibrations of H-O-H corresponding to the adsorbed water [24];
– 1032-1092 cm^{-1} – asymmetrical valence vibrations ν_1 of the PO_4^{3-} ion;
– 960 cm^{-1} – symmetrical valence vibrations ν_1 of the PO_4^{3-} ion;
– 560-600 cm^{-1} – asymmetrical deformation vibrations ν_4 of the PO_4^{3-} ion;
– 470 cm^{-1} – deformation vibrations ν_2 of the PO_4^{3-} ion.

In the stoichiometric sample (sample 3) there are maxima at 1356 and 1385 cm^{-1} relating to the ν_3 vibrations of the carbonate ion [25] (it is probably associated with adsorption of carbon dioxide from the atmosphere on the sample surface during aging) and also at 830 cm^{-1} – ν_2 vibrations of the NO_3^- nitrate ion (it can be conditioned by the precursor remains in the end product) [26].

ν_2 vibrations of the CO_3^{2-} -group corresponding to the absorption band at 1400-1500 cm^{-1} are pronounced for the samples 1, 3-6. In the case of the initial samples, the presence of the maximum near 870-875 cm^{-1} is typical for the B-type substitutions.

Maximum at 874 cm^{-1} is present in the initial sample 5 that indicates the presence of carbonate ions in the B-position. After annealing at 600 °C one can observe a significant decrease in the intensity of this maximum as well as its shift towards 878 cm^{-1} , i.e. carbonate leaves B-position and appears in A-position. Further thermal treatment leads to its slight shift and increase implying the incorporation into B- and A-positions.

For the samples thermally treated at 600 and 900 °C and obtained in synthesis 5 one can observe the following features typical for HA, which indicate the improvement of HA structuring as a result of thermal treatment: the appearance of the maxima in the vicinity of 3570 cm^{-1} and 630 cm^{-1} relating, respectively, to the valence and libration vibrations of the hydroxyl group as well as to the improvement of the absorption band appearance at 1090 cm^{-1} relating to the asymmetrical valence vibrations ν_1 of the PO_4^{3-} ion [27].

3.4 Analysis of the TECR data

The maximum CO_2 yield (see Fig. 9) is observed in the pair 2, 5. Therefore, one can suggest that these synthesis types lead to the inclusion of the maximum amount of carbonate ions in the samples structure. At that, synthesis itself is of a greater importance, since it is aimed at the production of the B-type carbon apatite (reaction equation 3) than the order of introduction of reagents which differs in the pair 2, 5. One can state that synthesis 2 is more preferred, since it results in the formation of carbon apatite without an additional rhenanite phase.

Carbon dioxide yield curve for the considered samples as well as for the sample 1 corresponds to the notions of thermal decomposition of CHA with a substantially lower CO_2 yield in the case of the latter [23].

Stoichiometric sample (No 3) liberates carbonate well at 680 °C. This low-temperature fraction, most likely, is

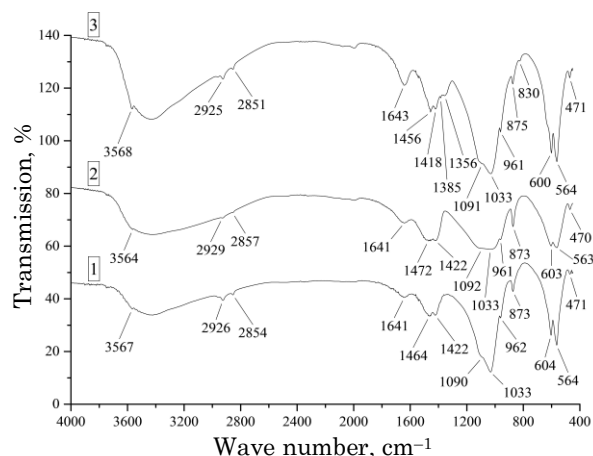


Fig. 6 – IR spectra of the samples 1-3

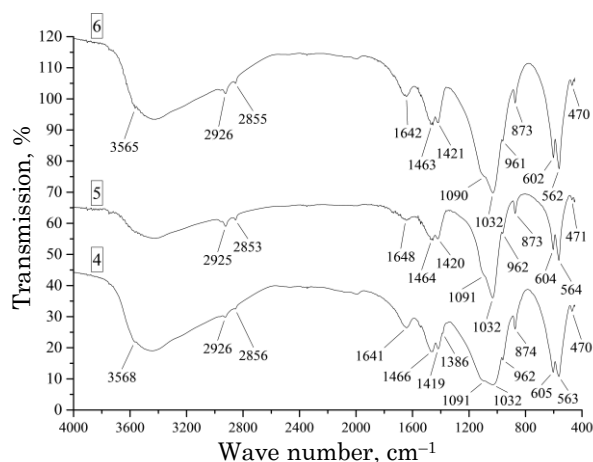


Fig. 7 – IR spectra of the samples 4-6

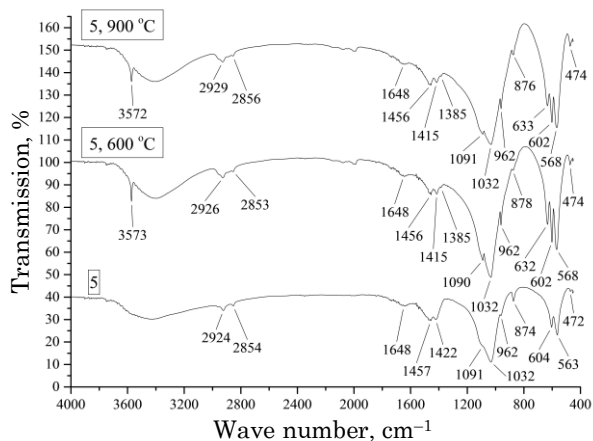
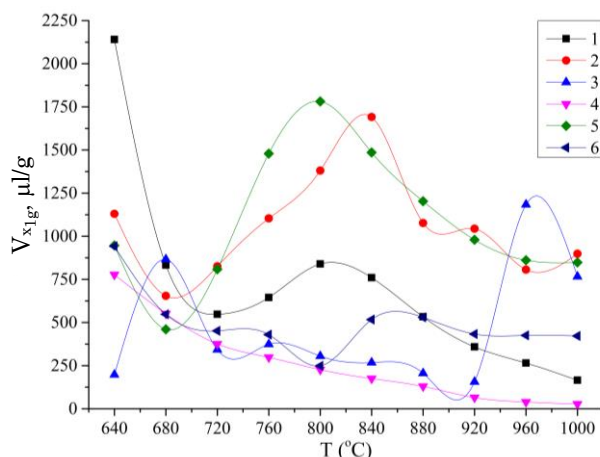


Fig. 8 – IR spectra of the initial and annealed at 600 °C and 900 °C sample 5

associated with carbonate ions of surface localization, but not with those incorporated into the crystal lattice. With further increasing temperature, CO₂ yield significantly decreases and indicates that intrinsic carbonate is absent in the CHA structure after thermal treatment at 700 °C. However, carbon dioxide emission from this sample shar-

Fig. 9 – CO₂ yield from the samples by the TEJR data

ply increases starting from 920 °C. Only CO₂ penetrated into the apatite structure from the reactor atmosphere at temperatures of 720-920 °C can be the source of this high-temperature fraction. Indirectly, this is also confirmed by a weaker crystallinity of this sample compared with CHA. The discovered feature indicates the possibility of CO₂ capture by the stoichiometric apatite lattice from the ambient atmosphere during its recrystallization.

Sample 4 shows a linear decrease in the escaping carbon dioxide with increasing temperature. Such behavior indicates poor embeddability of carbonate ions into the apatite structure. Another feature of the given sample is a substantial increase in the rhenanite phase with subsequent annealing at 900 °C.

For the sample 6, CO₂ yield at 840 °C increases and is constant in the sequel with increasing temperature.

4. CONCLUSIONS

The results of the investigation by the IRS, XRD and TEJR methods indicate the presence in all the samples in different amounts of carbonate ions with various preferred localization. The most optimal variant of synthesis (synthesis 2) was selected in order to obtain carbonate apatites without foreign phases.

Laws of the temperature evolution of CCA samples observed by TEJR, in particular, a significant CO₂ yield in a certain temperature range, indicate a substantial content in their structure of carbonate ions. Temperature behavior of the samples 1, 2, and 5 correlates well with previous studies of thermal decomposition of CHA [23] and also with the XRD and IRS results.

Atypical behavior of CO₂ release from some samples of carbonate apatites (for example, 3 and 6) can be associated with the structural features of these materials that will be the subject of further study.

Thus, the TEJR method and the experimental setup created for its implementation allow to investigate the temperature behavior of carbonate ions in apatites of different origin and make their quantitative assessment. The results obtained show that the combined use of XRD, IRS and TEJR provide a fairly complete characterization of synthetic and, in prospect, biological apatites.

REFERENCES

1. C. Rey, *Biomaterials* **11**, 13 (1990).
2. F. Betts, N.C. Blumenthal, A.S. Posner, *J. Cryst. Growth* **53**, 63 (1981).
3. R. Legros, N. Balmain, G. Bonel, *J. Chem. Res.(s)* **77**, 2313 (1986).
4. G. Montel, G. Bonel, J.C. Heughebaert, J.C. Trombe, C. Rey, *J. Cryst. Growth* **53**, 74 (1981).
5. C. Rey, B. Collins, T. Goehl, I.R. Dickson, M.J. Glimcher, *Calcified Tissue Int.* **45**, 157 (1989).
6. E. Landi, A. Tampieri, G. Celotti, L. Vichi, M. Sandri, *Biomaterials* **25**, 1763 (2004).
7. J.C. Elliott, *Structure and Chemistry of the Apatites and Other Calcium Orthophosphates* (Amsterdam: Elsevier: 1994).
8. A.A. Baig, J.L. Fox, R.A. Young, Z. Wang, J. Hsu, W.I. Higuchi, A. Chhetry, H. Zhuang, M. Otsuka, *Calcified Tissue Int.* **64**, 437 (1999).
9. T.I. Ivanova, O.V. Frank-Kamenetskaya, A.B. Kol'tsov, V.L. Ugolkov, *J. Solid State Chem.* **160**, 340 (2001).
10. R.Z. LeGeros, *Calcium phosphates in oral biology and medicine* (Basel: Karger: 1991).
11. A. Yasukawa, K. Kandori, T. Ishikawa, *Calcified Tissue Int.* **72**, 243 (2003).
12. L.D. Mkukuma, J.M.S. Skakle, I.R. Gibson, C.T. Imrie, R.M. Aspden, D.W. Hukins, *Calcified Tissue Int.* **75**, 321 (2004).
13. S.N. Danilchenko, V.A. Pokrovskiy, V.M. Bogatyrov, L.F. Sukhodub, B. Sulkio-Cleff, *Cryst. Res. Technol.* **40** No 7, 692 (2005).
14. S. Materazzi, S. Vecchio, *Appl. Spectrosc. Rev.* **46** No 4, 261 (2011).
15. *Calcium phosphates in biological and industrial systems* (Ed. Z. Amjad) (Boston: Kluwer Academic Publishers: 1998).
16. C.C. Kee, H. Ismail, A.F.M. Noor, *J. Mater. Sci. Technol.* **29** No 8, 761 (2013).
17. I.R. Gibson, W. Bonfield, *J. Biomed. Mater. Res.* **59**, 697 (2002).
18. J.-P. Lafon, E. Champion, D. Bernache-Assollant, R. Gibert, A.-M. Danna, *J. Therm. Anal. Calorim.* **72** No 3, 1127 (2003).
19. S. Jalota, S.B. Bhaduri, A.C. Tas, *J. Biomed. Mater. Res. B* **80** No 2, 304 (2007).
20. F.H. Chung, *J. Appl. Crystallogr.* **8**, 17 (1975).
21. H.P. Klug, L.E. Alexander, *X-Ray Diffraction Procedures: For Polycrystalline and Amorphous Materials* (New York: Wiley: 1974).
22. S.N. Danilchenko, O.G. Kukharenko, C. Moseke, I.Yu. Protsenko, L.F. Sukhodub, B. Sulkio-Cleff, *Cryst. Res. Technol.* **37** No 11, 1234 (2002).
23. A.B. Brik, S.N. Danilchenko, V.V. Radchuk, V.L. Karbovskij, A.M. Kalinichenko, N.N. Bagmut, *Mineral J.* **29** No 2, 32 (2007).
24. D. Tadic, F. Peters, M. Epple, *Biomaterials* **23**, 2553 (2002).
25. J.V. Rau, S. Nunziante Cesaro, D. Ferro, S.M. Barinov, I.V. Fadeeva, *J. Biomed. Mater. Res. B* **71B** No 2, 441 (2004).
26. S. Raynaud, E. Champion, D. Bernache-Assollant, P. Thomas, *Biomaterials* **23**, 1065 (2002).
27. A. Slosarczyk, Z. Paszkiewicz, C. Paluszkiwicz, *J. Mol. Struct.* **744**, 657 (2005).